Biosensors and Bioelectronics 35 (2012) 243–250

Contents lists available at SciVerse ScienceDirect

Biosensors and Bioelectronics

journal homepage: www.elsevier.com/locate/bios

Preparation of photolithographically patterned inverse opal hydrogel microstructures and its application to protein patterning

Yeongmin Lee [1], Sangphil Park [1], Sang Won Han, Tae Geuk Lim, Won-Gun Koh *

Department of Chemical and Biomolecular Engineering, Yonsei University, 134 Sinchon-Dong, Seodaemoon-Gu, Seoul 120-749, Republic of Korea

ARTICLE INFO

Article history:
Received 5 December 2011
Received in revised form 14 February 2012
Accepted 26 February 2012
Available online 3 March 2012

Keywords:
Protein pattern
Inverse opal hydrogel micropattern
Photopatterning
Biosensor

ABSTRACT

Protein pattern has played an important role in biosensors, bioMEMS, tissue engineering, fundamental studies of cell biology, and basic proteomics research. Here, we developed a straightforward and effective protein patterning technique using macroporous poly(2-hydroxyethyl methacrylate) (PHEMA) hydrogel micropatterns as a three-dimensional (3D) template for protein immobilization. Micropatterns of macroporous hydrogels with inverse opal structures were prepared on poly(ethylene glycol) (PEG)-coated silicon substrates by combining a colloidal crystal templating method with photopatterning. The resultant inverse opal hydrogel (IOH) micropatterns were modified with 3-aminopropyltriethoxysilane using the hydroxyl groups in PHEMA for the covalent immobilization of proteins. Proteins were selectively immobilized only on the hydrogel micropatterns, while the PEG regions served as an effective barrier to protein adsorption. Because of their highly ordered and interconnected 3D macroporous structures and large internal surface areas, protein loading in the IOH micropattern was about six times greater than that on a non-porous hydrogel micropattern, which consequently improved the protein activity. The porosity of the hydrogel micropatterns could be controlled using different sizes of colloidal nanoparticles, and using smaller nanoparticles produced hydrogel micropatterns with higher protein loading capacities and activities. To demonstrate the potential use of IOH micropatterns in biosensor systems, biotin was micropatterned on the hydrogels and the specific binding of streptavidin was successfully assayed using IOH micropatterns with better fluorescence signals and sensitivity than that of the corresponding non-porous hydrogel micropatterns.

1. Introduction

Since MacAlear and Wehrung (1978) created protein patterns to integrate protein molecules into bioelectronic microcircuits, protein patterning has become critical to basic biological research involving cell biology, high-throughput proteomic arrays and combinatorial library screening as well as conventional biosensor applications (Ito, 1999; Kane et al., 1999; MacBeath and Schreiber, 2000; Mitchell, 2002; Ostuni et al., 2001; Templin et al., 2003; Veiseh et al., 2002; Zhou et al., 2001; Zhu et al., 2000). Protein patterning is characterized by protein immobilization at specific locations in a two- or three-dimensional space at a micro- or nano-meter scale. Protein patterning has been performed by the selective attachment of proteins within designated regions in a substrate surrounded by a background region that is resistant to the adsorption of proteins and other molecules (Blawas and Reichert, 1998). A variety of methods have been explored previously for protein localization, including photolithography (Orth et al., 2003; Veiseh et al., 2002), photochemical fixation (Balakirev et al., 2005; Hengsakul and Cass, 1996), soft lithography (Hyun and Chilkoti, 2001; Whitesides et al., 2001), dip-pen lithography and related scanning probe patterning methods (Hyun et al., 2002; Lee et al., 2002), focused-ion-beam patterning and nanoimprint lithography (Hoff et al., 2004; Jiang et al., 2008). Most protein patterns have been generated on two-dimensional (2D) hard substrates such as glass, silicon, and gold through non-specific adsorption or covalent binding to the monolayer of tethered functional groups on the surfaces. However, the limited surface area of simple planar substrates limits the amount of protein that can be attached. Furthermore, immobilized proteins may become dehydrated and denatured due to rapid evaporation of the liquid environment and close contact with hard substrates, eventually losing their native structures and functions.

Several approaches were used to increase the amount of immobilized proteins by developing three-dimensional (3D) surfaces using porous substrates, nanofibers or the assembly of micro/nanoparticles (Kang et al., 2005; Lee et al., 2011; Son et al., 2011; Stewart and Buriak, 2000; Yang et al., 2009; Zhang, 2006).

* Corresponding author at: Department of Chemical and Biomolecular Engineering, Yonsei University, 134 Sinchon-Dong, Seodaemoon-Gu, Seoul 120-749, Republic of Korea. Tel.: +82 2 2123 5755; fax: +82 2 312 6401.
E-mail address: wongun@yonsei.ac.kr (W.-G. Koh).
[1] These authors contributed equally to this work.

0956-5663/$ – see front matter © 2012 Elsevier B.V. All rights reserved.
doi:10.1016/j.bios.2012.02.056

Protein denaturation could be minimized by modifying the surfaces of solid substrates with a soft material layer such as dendrimer and polymeric multilayers, which can provide a "cushioning effect" as well as a large hydration volume at the surface (Ajikumar et al., 2007; Doh and Irvine, 2004; Pathak et al., 2004). Hydrogels, 3D crosslinked polymers that swell in water or other biological fluids, are another attractive support material for protein immobilization, because the soft and hydrated environment of a swollen hydrogel can provide proteins with near-physiological conditions that minimize denaturation and help them to carry out their full biological functions (Zhang, 2004). Protein patterns were generated by encapsulating proteins within hydrogel micropatterns or immobilizing proteins onto the surfaces of hydrogels (Kim et al., 2008; Kiyonaka et al., 2004; Revzin et al., 2001; Russell et al., 1999; Tanase et al., 2011; Zourob et al., 2006). In the former case, diffusion limitation can interrupt the interactions between encapsulated proteins and other molecules; while in the latter case, the amount of immobilized protein cannot be dramatically increased compared to conventional hard materials.

To overcome above problems related with hydrogel-based protein patterning, we fabricated macroporous poly(2-hydroethyl methacrylate) (PHEMA) hydrogel micropatterns and used their surfaces as templates for protein patterning with the expectation that porous hydrogel could provide higher immobilization capacity and a more aqueous environment for immobilized proteins as compared to a two-dimensional hard surface. By combining a colloidal crystal templating method with nanoparticles and photopatterning, we fabricated hydrogel micropatterns that had three-dimensional (3D) inverse opal structures with highly ordered and interconnected pores of uniform size. After confirming that macroporous hydrogel micropatterns accommodated more proteins and exhibited better protein activity compared with nonporous hydrogel micropatterns, the feasibility of macroporous hydrogel micropatterns for biosensor applications was investigated.

2. Experimental

2.1. Materials

Styrene, potassium persulfate (KPS), 2-hydroethyl methacrylate (HEMA), ethylene glycol dimethacrylate (EGDMA), 2-hydroxy-2-methylpropiophenone (HOMPP), 3-aminopropyltriethoxysilane (APTES), bovine serum albumin (BSA) and BSA conjugated with fluorescein isocyanate (FITC-BSA) were purchased from Sigma–Aldrich (Milwaukee, WI, USA). Ethyl alcohol, chloroform and aqueous ammonia were purchased from Duksan Chemicals (Seoul, Korea). Glutaraldehyde (GA) (25% in solution) was purchased from Junsei Chemical (Tokyo, Japan). Biotinyl-3,6,9-dioxaoctanediamine (biotin-NH_2), prostate-specific antigen (PSA), anti-PSA antibody (anti-PSA), and a micro-BCA protein assay kit were obtained from Pierce (Rockford, IL, USA). FITC-labeled streptavidin (FTIC-SA) was purchased from Biosource (Camarillo, CA, USA). A chrome sodalime photomask for photolithographic patterning of hydrogels was designed to contain 200 μm circles arranged into a 50 × 50 array format and was purchased from Advanced Reproductions (Andover, MA, USA).

2.2. Equipment

Photopolymerization of the hydrogel precursor was performed using a 365 nm, 300 mW/cm^2 UV light source (EXFO Omnicure UV spot lamp, Mississauga, Ontario, Canada). Surface modifications were monitored by X-ray photoelectron spectroscopy (XPS) (Kratos Analytical Inc., Chestnut Ridge, NY, USA). Absorbance was measured using a VersaMax tunable microplate reader (Molecular Devices, Sunnyvale, CA, USA). Pattern morphology was observed with scanning electron microscopy (S-800, Hitachi, Tokyo, Japan). A microscope equipped with an integrated color CCD camera (BX-51, Olympus, Tokyo, Japan) was used to obtain optical and fluorescence images. Image analyses were performed using commercially available image analysis software (TOMORO Capture 2.0, Olympus). Confocal slice images were obtained using confocal microscopy (LSM 510 META, Carl Zeiss Inc., Thornwood, NY, USA). The *z*-average size of the PSNPs was measured suing a nanometer sized test instrument (model 2S, NanoS, Malvern Instruments, UK).

2.3. Synthesis of polystyrene nanoparticles

Polystyrene nanoparticles (PSNPs) were synthesized by dispersion polymerization. Water (400 mL), NH_3 stabilizer and styrene monomer (20 mL) were added to the double jacket reactor under a stirring speed of 500 rpm. After a solution of KPS initiator (0.25 g) pre-dissolved in water (25 mL) was added to the reactor, the polymerization proceeded for 8 h. The solid content of the synthesized polystyrene (PS) latex was 2.77 wt%. The PS latex was washed by centrifugation and dispersion with water, and was adjusted to a concentration of 20 mg/mL before use. The size of the PSNPs could be tuned in the range of 160–400 nm by varying the amount of NH_3 stabilizer. In this study, PSNPs with average diameters of about 160 nm, 180 nm, 240 nm and 400 nm were used. The amount of NH_3 stabilizer to tune PSNPs and size dispersion of each PSNP was shown in Table S1 and Fig. S1, respectively (see Supplementary material).

2.4. Micropatterns of inverse opal hydrogel

Fig. 1 describes the overall process for preparing micropatterns of inverse opal hydrogel (IOH) based on PHEMA. First, PSNPs (160 nm, 180 nm, 240 nm or 400 nm) were self-assembled onto silicon wafers (1.5 cm × 1.5 cm) via a meniscus evaporation procedure. To form close-packed colloidal crystal templates, we evaporated the aqueous solvent in the colloidal suspension at 80 °C for 40 min in a thermostatic chamber after 400 μL of colloidal suspension were deposited onto the silicon wafers. Silicon substrates were surface-modified with PEG by a previously described method to minimize non-specific adsorption (Papra et al., 2001). After that, 100 μL of PHEMA hydrogel precursor solution, consisting of HEMA, 1 wt% of EGDMA as a crosslinker and 2 wt% of HOMPP as an initiator, were dropped onto the colloidal templates, and were then spin-coated for 40 s at 3000 rpm to generate a thin layer of precursor solution with uniform thickness. This layer was covered with the photomask we designed and exposed to UV light for 25 s through the photomask. Upon exposure to UV light, only the exposed regions underwent free-radical-induced gelation and became insoluble in water. As a result, the desired microstructures were obtained by washing away the unreacted precursor solution with water. Finally, substrates containing hydrogel micropatterns were immersed in chloroform for 3 min to completely remove the hydrogel-embedded PSNPs and create inverse opal structures within the hydrogel micropatterns. As a control experiment, nonporous PHEMA micropatterns were fabricated using the same photolithography process except for the steps involving the deposition and removal of PSNPs.

2.5. Protein immobilization on the hydrogel micropatterns

A silanization reaction was used for surface modification of PHEMA hydrogel micropatterns (both non-porous and inverse opal hydrogels) by utilizing the hydroxyl groups in the PHEMA. Hydrogel micropatterns were immersed in 3% (v/v) APTES in 95% (v/v) ethanol under a nitrogen environment for 2 h at room

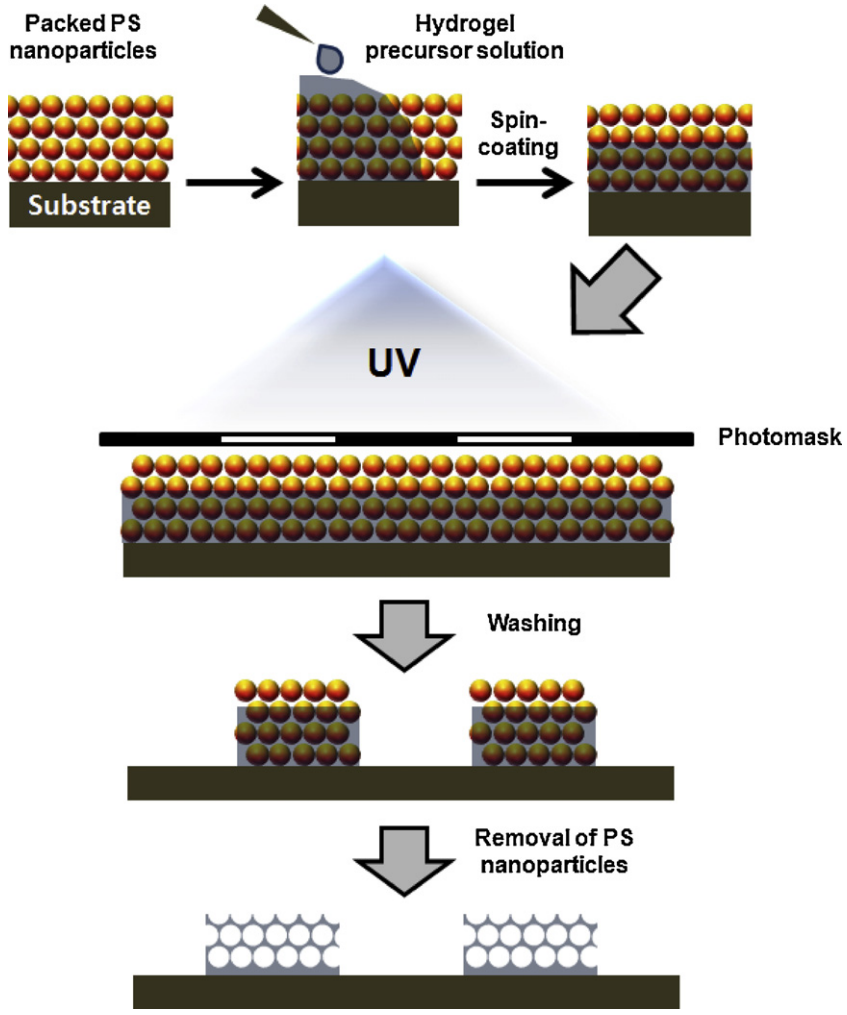

Fig. 1. Schematic illustration of fabricating micropatterns of inverse opal hydrogel based on PHEMA.

temperature, and then washed with ethanol to remove non-covalently bound APTES. APTES-modified hydrogel patterns were reacted with a 2.5% (v/v) solution of glutaraldehyde in PBS for 2 h at room temperature to activate the amine groups in the APTES, and then incubated with FITC-BSA (1 mg/mL), glucose oxidase (1 mg/mL) or biotin-NH_2 (0.1 mg/mL) solution for 24 h at 4 °C. The resultant protein-immobilized hydrogel micropatterns were washed with PBS for 24 h to remove non-covalently attached proteins. The amount of immobilized proteins was quantified by measuring the initial and final concentrations of the proteins in the incubation solution using a BCA standard working agent.

2.6. Determination of protein activity

The activity of glucose oxidase (GOX) immobilized on the micropatterns was determined in a colorimetric assay of hydrogen peroxide formed by the oxidation of *o*-dianisidine through a peroxidase-coupled system. Each reaction contained 2.4 mL of *o*-dianisidine solution (0.21 mM in deionized water, pH 7.4), 0.1 mL of β-D-glucose solution (20 mg/mL in DI water), and 0.1 mL of peroxidase solution (1 mg/mL in PBS buffer). These solutions were added to the micropattern-immobilized GOX and allowed to react at 37 °C. The reaction was stopped by the addition of 0.5 mL of 2.5 M sulfuric acid, and quantified by measuring the absorbance at 405 nm in a UV spectrophotometer.

2.7. Study of streptavidin and biotin system

Hydrogel micropatterns were used to study the molecular recognition between biotin and streptavidin. A 10 mM solution of biotin-NH_2 in PBS was directly coupled to the APTES-modified PHEMA micropattern via the same procedure described above. After patterning of biotin-NH_2 on the hydrogel, the hydrogel micropatterns were incubated with different concentrations of FITC-SA solution for 10 min. The binding of streptavidin to micropatterned biotin was visualized and quantified using fluorescence microscopy.

2.8. Detection of PSA

Hydrogel micropatterns were reacted with a 20 ng/mL solution of anti-PSA in PBS for 2 h at room temperature. After immobilization of anti-PSA, hydrogel micropatterns were blocked with BSA solution (1 wt% BSA in PBS solution) for 2 h, and subsequently reacted with different concentrations of PSA for 2 h at room temperature. To perform immunoassays, we used sandwich immunoassays with fluorescence-labeled antibodies. We used the Alexa Fluor 488 Monoclonal antibody labeling kit, and labeled anti-PSA with Alexa 488 as described in the manufacturer's protocol (http://probes.invitrogen.com/media/pis/mp20181.pdf). After the reaction between anti-PSA and PSA, 20 ng/mL solution of fluorescence-labeled anti-PSA in PBS was introduced to the

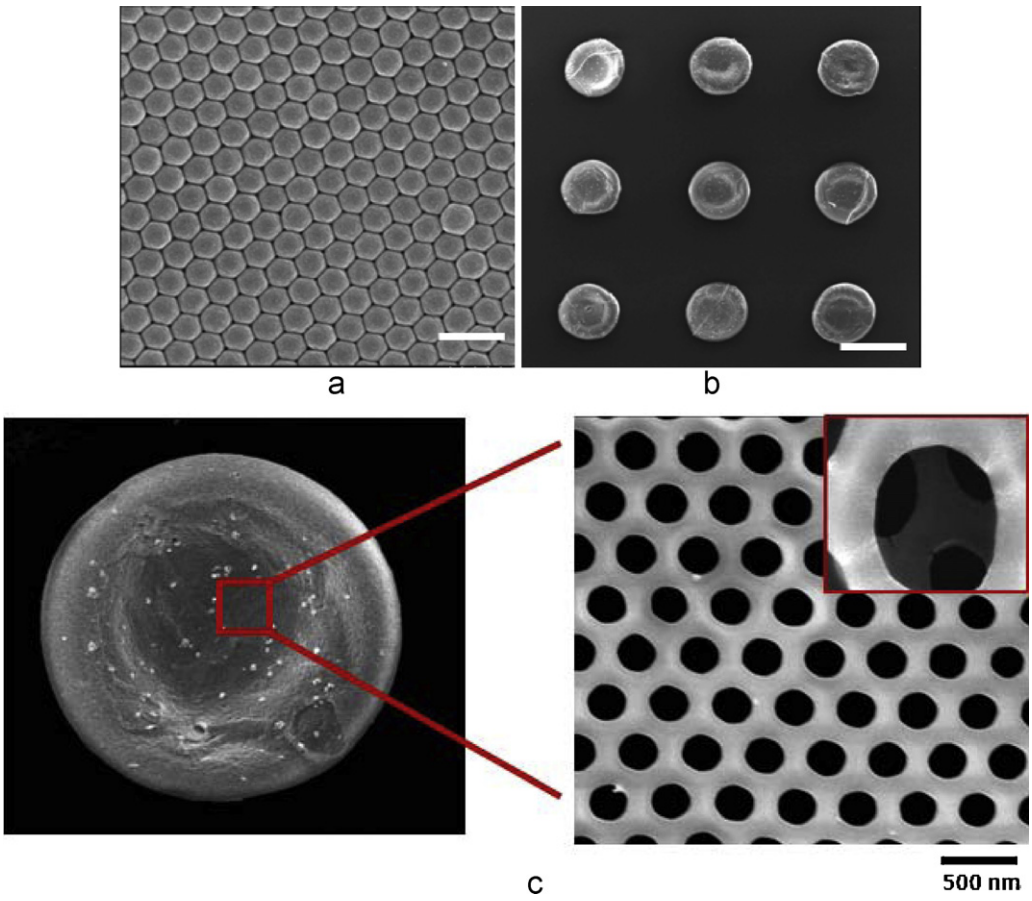

Fig. 2. SEM images of (a) PS opal template of a colloidal crystal template with a diameter of 240 nm (scale bar: 500 nm) and (b) microarray of inverse opal PHEMA hydrogel (scale bar: 200 μm). (c) High magnification SEM images of inverse opal hydrogel micropatterns with a highly ordered and interconnected 3D macroporous structure.

substrate surface and incubated for 2 h. The substrate was rinsed with PBS and dried under a nitrogen environment and fluorescence intensities were measured.

2.9. Statistics

We compared statistically significant difference between different IOH micropatterns (four different pore sizes, 160, 180, 240, and 400 nm). Here, five samples ($n = 5$) are represented for each data. Data were compared using an independent two-sample t-test, and P values less than 0.005 were considered statistically significant.

3. Results and discussion

In this study, micropatterns of macroporous hydrogels with inverse opal structures were prepared by combining a colloidal crystal templating method with photopatterning. Closely packed multi-layered assemblies of PS nanoparticles with approximately 70-μm thicknesses were formed on PEG-modified silicon substrates based on a combination of the sedimentation of spherical particles in dispersion liquid and the evaporation of the dispersion, as described in previous studies (Fig. 2a) (Lee et al., 2004; Nagao et al., 2007). After the infiltration of the hydrogel precursor solution and subsequent spin-coating, photopatterning was performed, followed by removal of the PS templates. Here, proximity photolithography was used to generate hydrogel micropatterns because mask contact with colloidal templates can disrupt the closely packed structure of the template. As shown in Fig. 2b, a clearly defined array of hydrogel microstructures was successfully fabricated with no residual PS nanoparticles or hydrogel on the non-exposed area of the substrate. The height of the hydrogel micropatterns was approximately 50 μm, which was lower than that of the PS templates, due to the spin-coating process. The spin-coating step made the precursor solution thinner than that of the PS template, preventing the PS template from being covered by the precursor solution and thereby ensuring the formation of an IOH with a highly ordered and interconnected 3D macroporous structure and large internal surface area as shown in Fig. 2c. The resultant macroporous hydrogel micropatterns remained on the PEG-modified surface without detaching from the substrate when exposed to an aqueous environment for a week. However, for the long term (several weeks or months) used of protein microarrays, we are suggesting the use of acrylate-terminated methoxysilanes with PEG-terminated silane as reported by Revzin et al. because acrylate moieties served to covalently anchor hydrogel micropatterns to silicon substrates, resulting in permanent attachment of hydrogel to the surface (Seo et al., 2011).

We used macroporous IOH micropatterns as a support to immobilize proteins for the purpose of creating 3D protein patterns. For the covalent immobilization of proteins, PHEMA hydrogels were modified with APTES to provide amine groups that could serve as sites for the immobilization of proteins. XPS analysis revealed that new N 1s signals not present in the unmodified PHEMA hydrogel were observed for the APTES-modified hydrogel, confirming the successful incorporation of APTES into the PHEMA hydrogel as shown in Fig. S2 (see supplementary material). This result also confirmed that almost no protein could physically adsorb onto unmodified PHEMA hydrogel. Using the glutaraldehyde reaction, the amine groups in APTES were converted to aldehyde groups that could react with other amine groups in

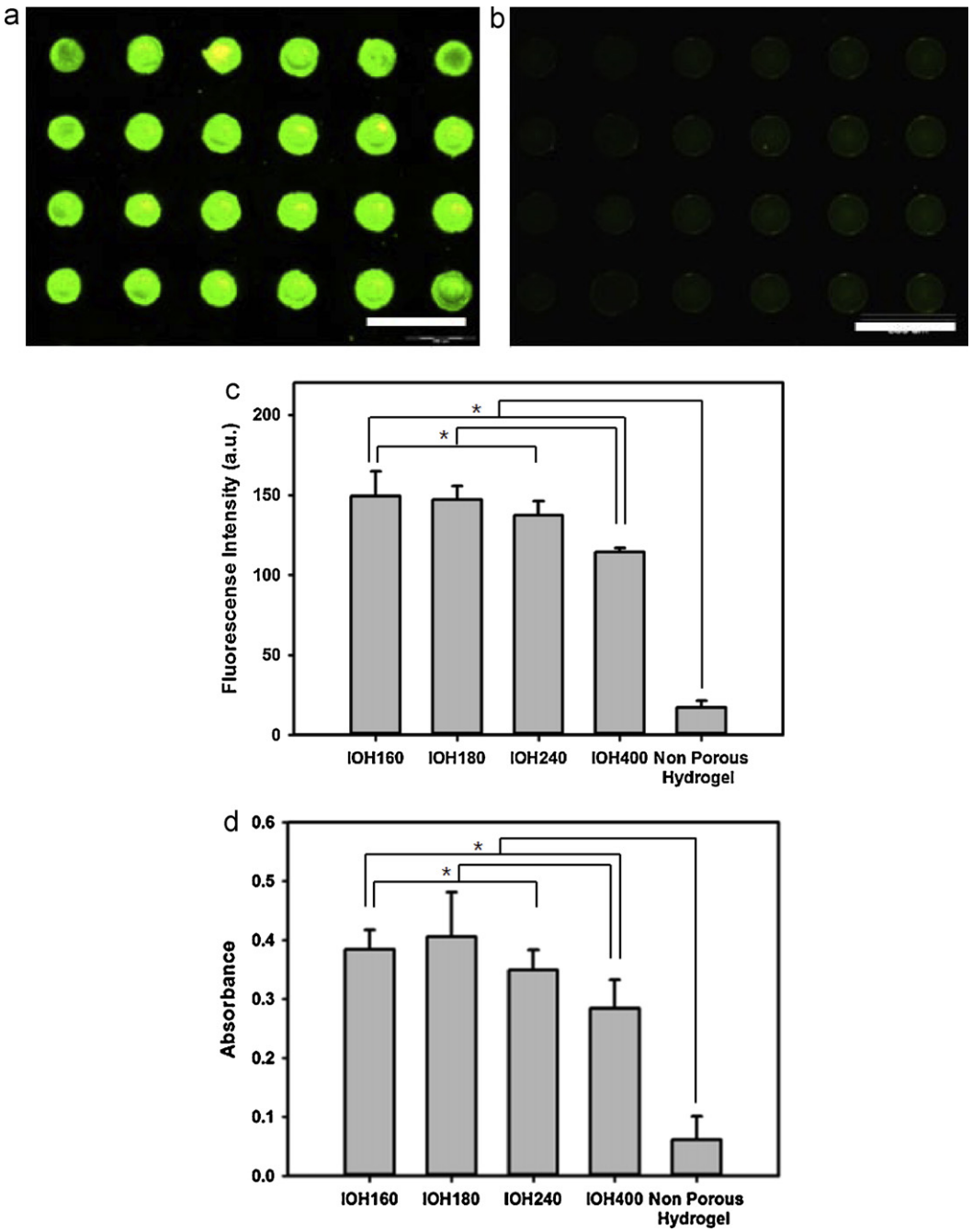

Fig. 3. Fluorescence images of micropatterned (a) inverse opal hydrogel (IOH 240) and (b) non-porous hydrogel that were incubated with FITC-BSA. (c) Fluorescence intensities of different micropatterns immobilizing FITC-BSA. (d) Relative activity of glucose oxidase immobilized on different micropatterns (Error bars represent means ± standard deviation. Asterisks denote statistically significant difference ($P < 0.005$) between different IOH micropatterns.).

proteins to form a stable imine linkage. Because the PEG layers on the glass surface were non-adhesive to proteins, micropatterning of the APTES-modified PHEMA hydrogels created a clear contrast between the adhesion-promoting hydrogel micropattern and the adhesion-resisting PEG-coated surface. The feasibility of selectively immobilizing proteins on the micropatterned IOH was investigated by incubating FITC-BSA with the micropatterned substrate to visualize the localization and patterning of the protein. Fig. 3a shows a fluorescence image of micropatterned substrates incubated with FITC-BSA, where the fluorescent and dark regions correspond to the IOH micropattern regions with immobilized BSA and the PEG hydrogel regions, respectively. These results indicate that albumin was immobilized only onto the IOH micropatterns, with the PEG hydrogel serving as an effective barrier to albumin adsorption, demonstrating that the spatial control of protein immobilization was possible using IOH micropatterns on PEG-coated surfaces. FITC-BSA was also immobilized on APTES-modified non-porous PHEMA hydrogel micropatterns so we were able to compare the protein-loading capacities of the IOH and non-porous micropatterns. As shown in Fig. 3b, the non-porous hydrogel micropatterns emitted much weaker fluorescence signals than the IOH micropatterns. The relative amounts of immobilized proteins were determined from the quantitative fluorescence intensity data (Fig. 3c). Because of the increased surface area of the highly ordered and interconnected 3D macroporous structure, the IOH hydrogel micropatterns bound more protein and subsequently emitted stronger fluorescence signals than the corresponding non-porous micropatterns. Among the IOH hydrogel micropatterns, the IOH

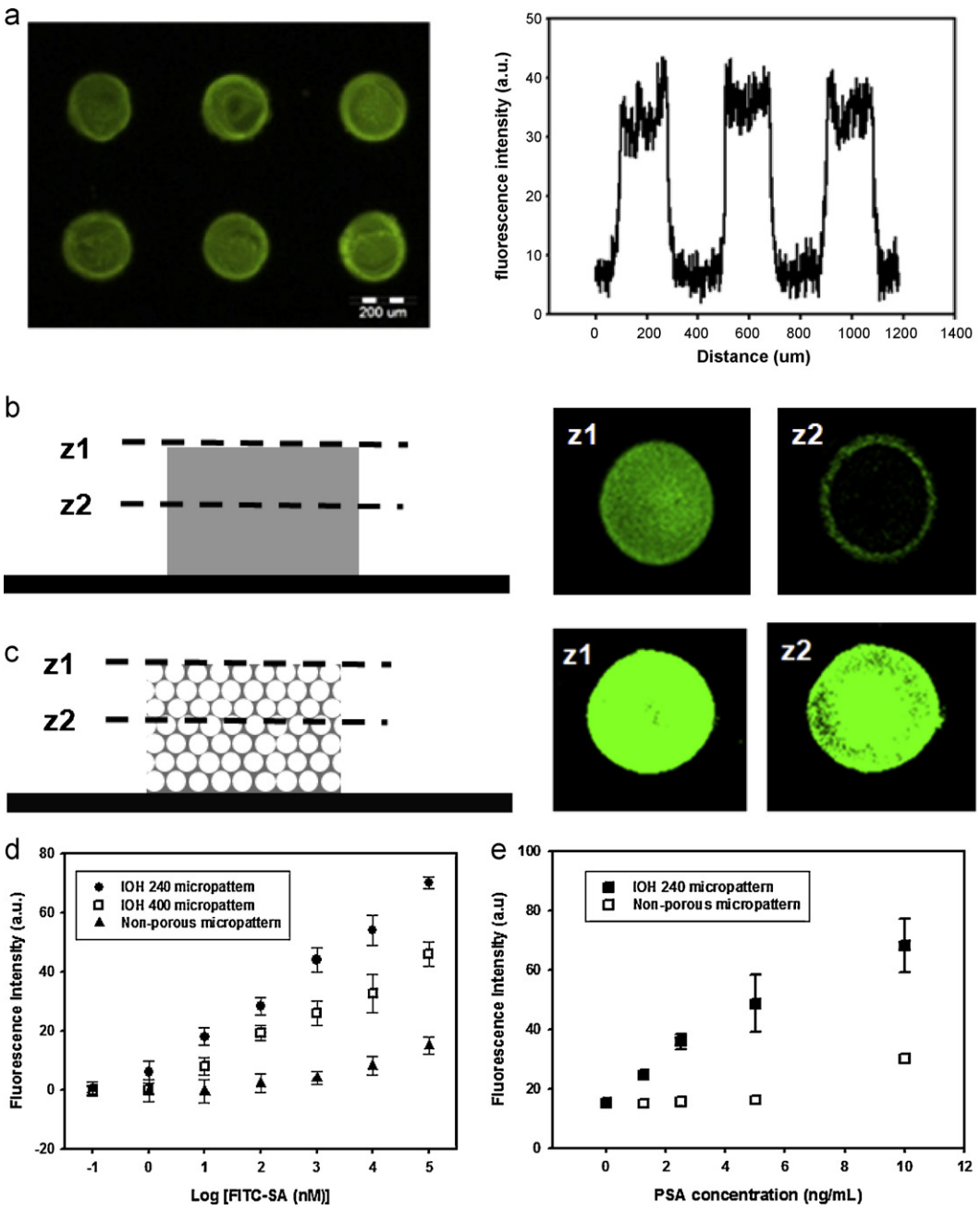

Fig. 4. Bioassay using micropatterned inverse opal hydrogels. (a) Fluorescence image and intensity profile of FITC-SA bound to biotin immobilized onto inverse opal hydrogel (IOH 240) micropatterns. Confocal slice images of (b) non-porous hydrogel and (c) inverse opal hydrogel (IOH 240) micropatterns at two different height positions ($z1$, $z2$). (d) Relationship between concentration of FITC- SA and the fluorescence intensity. (e) Relationship between concentration of PSA and the fluorescence intensity.

micropatterns made from the 240-nm PSNPs (IOH 240) showed stronger fluorescence intensity than those made from the 400-nm PSNPs (IOH 400) due to their higher porosity. However, there was no significant increase in fluorescence intensity as pore size of IOH micropatterns decreased from 240 nm to 180 nm and 160 nm. A BCA protein assay revealed that the actual amounts of immobilized protein were $43.23 \pm 6.54\,\mu g/cm^2$, $34.24 \pm 5.65\,\mu g/cm^2$ and $6.28 \pm 1.10\,\mu g/cm^2$ for the IOH 240, IOH 400 and non-porous hydrogel micropatterns, respectively. Without APTES modification, $1.30 \pm 0.35\,\mu g/cm^2$ and $0.97 \pm 0.24\,\mu g/cm^2$ of BSA existed in IOH 240, and IOH 400 micropatterns, indicating that almost no protein could physically adsorb on the PHEMA hydrogel, but could be immobilized on the PHEMA hydrogel only through the covalent bonding via APTES. We also investigated the activities of proteins immobilized onto different hydrogel micropatterns, using GOX as a model protein. The activity of immobilized GOX was assessed with a colorimetric assay based on the oxidation of *o*-dianisidine in a POD-coupled system. Fig. 3d shows that the higher absorbance was observed for IOH micropatterns than non-porous hydrogel micropatterns and a similar trend was obtained for protein activity with the amount of immobilized proteins. Although high surface density is not necessarily related to high activity due to the possible hindrance of access of target molecules by steric interference between immobilized proteins, these results indicates that the higher binding capacity of the porous structures resulted in the enhancement of enzyme activity in the IOH micropatterns. It was

expected that the high density and activity of immobilized proteins would increase the signal-to-noise ratio and lower the detection limit in protein-based biosensor applications.

To demonstrate the potential use of IOH micropatterns in biosensor systems, we investigated the specific binding between biotin and streptavidin (SA) mediated by molecular recognition. The biotin–streptavidin system was chosen for our experiments because it provides a universal platform for patterning a variety of biomolecules. Biotin-NH_2 was covalently immobilized onto the APTES-modified hydrogel micropatterns, and the resultant micropatterned substrates were incubated with FITC-SA. Fluorescent images demonstrated that streptavidin specifically bound to the biotin-immobilized macroporous IOH microdomains and that nonspecific adsorption was insignificant in the PEG regions (Fig. 4a). The fluorescence intensity of the biotin–streptavidin micropatterns was nearly identical at each binding site, indicating that the densities of binding sites at each micropatterned location were similar. The location of the immobilized FITC-SA was further investigated with confocal microscopy. Fig. 4b and c shows the slice images of a biotin-immobilized IOH and the non-porous hydrogel micropatterns that reacted with FITC-SA, where slice images were obtained at two different height positions (z). In the case of the non-porous hydrogel micropattern, most of the FITC-SA was bound to the sidewall as well as to the top of the hydrogel microstructure. The mesh size of the hydrogel was not large enough to fully permit the diffusion of FITC-SA into the hydrogel microstructure, resulting in the binding of FITC-SA only in the outer region of the hydrogel micropatterns, leaving empty space inside the hydrogel microstructures (Fig. 4b). According to previous studies, mesh size of PHEMA hydrogel and dimension of streptavidin was 1.62 nm × 3.56 nm and was 6 nm × 5 nm × 5 nm, respectively (Hemming et al., 1995; Peppas et al., 1985). In contrast, FITC-SA was bound to all of the regions of the IOH micropatterns due to their highly ordered and interconnected macroporous structures (Fig. 4c). The capability to bind more FITC-SA provided IOH micropatterns with a stronger fluorescence signal and subsequently enhanced sensitivity and detection limits relative to the non-porous hydrogel micropatterns. Fig. 4d shows the changes in fluorescent intensity in three different hydrogel micropatterns (IOH 240, IOH 400 and non-porous) as a function of FITC-SA concentration. Here, fluorescence intensity values were obtained after subtracting the fluorescence intensity value of a solution without FITC-SA. The fluorescence intensity increased with increasing concentrations of FITC-SA, and the detection limit and sensitivity (change in signal per change in concentration) were enhanced in the IOH micropatterns (IOH 240 showed better performance than IOH 400) compared to the non-porous hydrogel micropatterns, as expected from the results of the protein loading density and activity data. The detection limits of FITC-SA were about 1.0 nM, 10.0 nM, and 100 nM for IOH 240, IOH 400, and non-porous hydrogel micropatterns, respectively, while sensitivity were about 0.7 μM^{-1}, 0.46 μM^{-1}, and 0.15 μM^{-1} for IOH 240, IOH 400, and non-porous hydrogel micropatterns, respectively.

After confirming that using IOH micropatterns provides enhanced sensitivity and detection limits compared to non-porous hydrogel for use in affinity-based biosensing, we carried out immunoassays using IOH micropatterns to detect PSA. PSA is a member of the kallikrein family that is exclusively produced by the prostate gland and has a concentration of 0–4 ng/mL in normal serum (Catalona et al., 1996). Prostate cancer and other pathological prostatic changes may cause PSA to leak into the peripheral circulation and induce abnormal elevations of serum PSA. PSA concentrations higher than 4 ng/mL may suggest prostate cancer. Fig. 4e shows the relationship between PSA concentrations and fluorescence intensity for IOH and non-porous hydrogel. This figure quantitatively demonstrates that IOH can produce higher fluorescence signals and sensitivity than non-porous hydrogel, because 3D macroporous systems yield increased densities of antibody binding sites and activity.

Although several groups reported IOH-based sensors, most of them were based on a change in optical properties of bulk IOH that was resulted from swelling and shrinking of hydrogel by external stimuli (Hu et al., 2007, 2008; Wang et al., 2007). We would like to emphasize that this is the first reports of fabricating protein-immobilizing micropatterned IOH that can be potentially utilized for various biomedical applications.

4. Conclusion

We fabricated macroporous hydrogel micropatterns and used them as templates for protein patterning. The combination of a colloidal crystal templating method with PS nanoparticles and photopatterning produced IOH micropatterns with highly ordered and interconnected 3D macroporous structures. A protein-repellent PHEMA hydrogel surface was modified with APTES to covalently attach proteins to the hydrogel surface. Because of their large internal surface areas, the IOH micropatterns exhibited higher protein loading capacities and greater activities than the corresponding non-porous hydrogel micropatterns. To evaluate a potential biosensor application, specific binding assays between streptavidin and biotin were successfully carried out using IOH micropatterns with better sensitivity and detection limits than those of non-porous hydrogel micropatterns. In the future, IOH micropatterned substrates could be combined with microprinting systems that locate different proteins into specific microdomains to develop protein microarrays containing different proteins capable of multiplexed protein-based assays.

Acknowledgments

This work was supported by the National Research Foundation (NRF) grant funded by the Ministry of Education, Science and Technology (MEST) (2011-0022709, 2010K001430 “Converging Research Center Program”, and R11-2007-050-03002-0 “Active Polymer Center for Pattern Integration at Yonsei University”).

Appendix A. Supplementary data

Supplementary data associated with this article can be found, in the online version, at doi:10.1016/j.bios.2012.02.056.

References

Ajikumar, P.K., Kiat, J., Tang, Y.C., Lee, J.Y., Stephanopoulos, G., Too, H.P., 2007. Langmuir 23, 5670–5677.
Balakirev, M.Y., Porte, S., Vernaz-Gris, M., Berger, M., Arie, J.P., Fouque, B., Chatelain, F., 2005. Anal. Chem. 77, 5474–5479.
Blawas, A.S., Reichert, W.M., 1998. Biomaterials 19, 595–609.
Catalona, W.J., Hudson, M.A., Scardino, P.T., Riche, J.P., Ahmann, F.R., Flanigan, R.C., deKernion, J.B., Ratliff, T.L., Kavoussi, L.R., Dalkin, B.L., Waters, W.B., MacFarlane, M.T., Southwick, P.C., 1996. J. Urol. 155, 1396.
Doh, J., Irvine, D.J., 2004. J. Am. Chem. Soc. 126, 9170–9171.
Hemming, S.A., Bochkarev, A., Darst, S.A., Kornberg, R.D., Ala, P., Yang, D.S.C., Edwards, A.M., 1995. J. Mol. Biol. 246, 308–316.
Hengsakul, M., Cass, A.E.G., 1996. Bioconjug. Chem. 7, 249–254.
Hoff, J.D., Cheng, L.J., Meyhofer, E., Guo, L.J., Hunt, A.J., 2004. Nano Lett. 4, 853–857.
Hu, X.B., Li, G.T., Huang, J., Zhang, D., Qiu, Y., 2007. Adv. Mater. 19, 4327–4332.
Hu, X.B., Li, G.T., Li, M.H., Huang, J., Li, Y., Gao, Y.B., Zhang, Y.H., 2008. Adv. Funct. Mater. 18, 575–583.
Hyun, J., Chilkoti, A., 2001. J. Am. Chem. Soc. 123, 6943–6944.
Hyun, J., Ahn, S.J., Lee, W.K., Chilkoti, A., Zauscher, S., 2002. Nano Lett. 2, 1203–1207.
Ito, Y., 1999. Biomaterials 20, 2333–2342.
Jiang, J., Li, X.M., Mak, W.C., Trau, D., 2008. Adv. Mater. 20, 1636–1643.
Kane, R.S., Takayama, S., Ostuni, E., Ingber, D.E., Whitesides, G.M., 1999. Biomaterials 20, 2363–2376.
Kang, M.C., Trofin, L., Mota, M.O., Martin, C.R., 2005. Anal. Chem. 77, 6243–6249.

Kim, D.N., Lee, W., Koh, W.G., 2008. Anal. Chim. Acta 609, 59–65.
Kiyonaka, S., Sada, K., Yoshimura, I., Shinkai, S., Kato, N., Hamachi, I., 2004. Nat. Mater. 3, 58–64.
Lee, K.B., Park, S.J., Mirkin, C.A., Smith, J.C., Mrksich, M., 2002. Science 295, 1702–1705.
Lee, Y.J., Pruzinsky, S.A., Braun, P.V., 2004. Langmuir 20, 3096–3106.
Lee, Y., Lee, H.J., Son, K.J., Koh, W.G., 2011. J. Mater. Chem. 21, 4476–4483.
MacAlear, J.M., Wehrung, J.M., 1978. Microsubstrates and method for making micropattern devices. US Patent.
MacBeath, G., Schreiber, S.L., 2000. Science 289, 1760–1763.
Mitchell, P., 2002. Nat. Biotechnol. 20, 225–229.
Nagao, D., Kameyama, R., Kobayashi, Y., Konno, M., 2007. Colloids Surf. A: Physicochem. Eng. Asp. 311, 26–31.
Orth, R.N., Clark, T.G., Craighead, H.G., 2003. Biomed. Microdev. 5, 29–34.
Ostuni, E., Chen, C.S., Ingber, D.E., Whitesides, G.M., 2001. Langmuir 17, 2828–2834.
Papra, A., Gadegaard, N., Larsen, N.B., 2001. Langmuir 17, 1457–1460.
Pathak, S., Singh, A.K., McElhanon, J.R., Dentinger, P.M., 2004. Langmuir 20, 6075–6079.
Peppas, N.A., Moynihan, H.J., Lucht, L.M., 1985. J. Biomed. Mater. Res. 19, 397–411.
Revzin, A., Russell, R.J., Yadavalli, V.K., Koh, W., Deister, C., Hile, D.D., Mellott, M.B., Pishko, M.V., 2001. Langmuir 17, 5440–5447.
Russell, R.J., Pishko, M.V., Simonian, A.L., Wild, J.R., 1999. Anal. Chem. 71, 4909–4912.
Seo, J.H., Chen, L.J., Verkhoturov, S.V., Schweikert, E.A., Revzin, A., 2011. Biomaterials 32, 5478–5488.
Son, K.J., Ahn, S.H., Kim, J.H., Koh, W.G., 2011. ACS Appl. Mater. Interfaces 3, 573–581.
Stewart, M.P., Buriak, J.M., 2000. Adv. Mater. 12, 859–869.
Tanase, C.P., Albulescu, R., Neagu, M., 2011. Expert Rev. Mol. Diagn. 11, 461–464.
Templin, M.F., Stoll, D., Schwenk, J.M., Potz, O., Kramer, S., Joos, T.O., 2003. Proteomics 3, 2155–2166.
Veiseh, M., Zareie, M.H., Zhang, M.Q., 2002. Langmuir 18, 6671–6678.
Wang, J.Y., Cao, Y., Feng, Y., Yin, F., Gao, J.P., 2007. Adv. Mater. 19, 3865–3871.
Whitesides, G.M., Ostuni, E., Takayama, S., Jiang, X., Ingber, D.E., 2001. Annu. Rev. Biomed. Eng. 3, 335–373.
Yang, D.Y., Liu, X., Jin, Y., Zhu, Y., Zeng, D.D., Jiang, X.Y., Ma, H.W., 2009. Biomacromolecules 10, 3335–3340.
Zhang, S., 2004. Nat. Mater. 3, 7–8.
Zhang, Y., 2006. Colloids Surf. B: Biointerfaces 48, 95–100.
Zhou, H.H., Roy, S., Schulman, H., Natan, M.J., 2001. Trends Biotechnol. 19, S34–S39.
Zhu, H., Klemic, J.F., Chang, S., Bertone, P., Casamayor, A., Klemic, K.G., Smith, D., Gerstein, M., Reed, M.A., Snyder, M., 2000. Nat. Genet. 26, 283–289.
Zourob, M., Gough, J.E., Ulijn, R.V., 2006. Adv. Mater. 18, 655–659.